Supplementary Information

Highly efficient CO_2 hydrogenation to long-chain linear α-olefins via CO intermediate enrichment over Na/FeMn/ZrO_2 catalysts

Kangzhou Wang[a,*], Tong Liu[b], Pengqi Hai[a], Shunnosuke Fujii[c], Chufeng Liu[c], Hanyao Song[c], Caixia Zhu[d], Guangbo Liu[d,e], Jianli Zhang[b,*], Zhou-jun Wang[b,f,*], Noritatsu Tsubaki[c,*]

[a] School of Materials and New Energy, Ningxia University, Yinchuan 750021, Ningxia, China.

[b] State Key Laboratory of High-efficiency Utilization of Coal and Green Chemical Engineering, College of Chemistry & Chemical Engineering, Ningxia University, Yinchuan 750021, Ningxia, China.

[c] Department of Applied Chemistry, School of Engineering, University of Toyama, Gofuku 3190, Toyama 930-8555, Japan.

[d] Qingdao Institute of Bioenergy and Bioprocess Technology, Chinese Academy of Sciences, Qingdao 266101, China.

[e] College of Chemical Engineering, Qingdao University of Science and Technology, 53 Zhengzhou Road, Qingdao 266042, China.

[f] State Key Laboratory of Chemical Resource Engineering, Beijing Key Laboratory of Energy Environmental Catalysis, Beijing University of Chemical Technology, Beijing, 100029, China.

*Corresponding author: kangzhou_wang@nxu.edu.cn (K. Wang); zhangjl@nxu.edu.cn (J. Zhang); wangzj@mail.buct.edu.cn (Z.-j. Wang); tsubaki@eng.u-toyama.ac.jp (N. Tsubaki)

1. Catalyst preparation

The Na/FeMn/ZrO_2 catalyst was prepared via a pre-coordination anchoring strategy. Typically, 2.02 g $Fe(NO_3)_3 \cdot 9H_2O$ (AR, Sinopharm Chemical Reagent Co., Ltd), 1.26 g $Mn(NO_3)_2 \cdot 6H_2O$ (AR, Sinopharm Chemical Reagent Co., Ltd), and 11.69 g ethylene diamine tetraacetic acid (AR, Sigma Aldrich) was dissolved into 37.28 g of deionized water under stirring to form a solution, to which 6.52 g of ZrO_2 (AR, Sinopharm Chemical Reagent Co., Ltd) was added with continuous stirring for 5 h. Subsequently, the mixture was heated to 120 ºC for evaporation and drying under stirring, and then calcined at 650 ºC for 6 h to obtain the FeMn/ZrO_2 sample. The Na/FeMn/ZrO_2 catalyst was fabricated by an impregnation method. In brief, 0.05 g Na_2CO_3 (AR, Sinopharm Chemical Reagent Co., Ltd) was dissolved into 2.0 g of deionized water. The resultant solution was added dropwise to 1.0 g of FeMn/ZrO_2 sample under ultrasonic condition. After drying in vacuum at 60 ºC for 12 h, the Na/FeMn/ZrO_2 catalyst was obtained. Unless specified otherwise, Na and FeMn loading were fixed at 2 wt% and 30 wt%, respectively. The ZrO_2 used in the aforementioned catalysts is monoclinic ZrO_2.

The reference of Na/FeMn/SiO_2 catalysts were prepared using pre-coordination anchoring strategy. The pre-coordination anchoring strategy primarily involved the formation of metal complexes through ligand-metal ion coordination. The carboxyl groups on the complex surface esterify with hydroxyl groups on the support surface, anchoring the metal ions to the support. Subsequently, reduction and carbonization treatments were applied to form the interfacial structure. In brief, a certain amount of $Fe(NO_3)_3 \cdot 9H_2O$ (AR, Sinopharm Chemical Reagent Co., Ltd), $Mn(NO_3)_2 \cdot 6H_2O$ (AR, Sinopharm Chemical Reagent Co., Ltd), ethylene diamine tetraacetic acid (AR, Sigma Aldrich) were dissolved into deionized water under stirring. Then,

SiO_2 (AR, Sigma Aldrich) was added to the above solution with continuous stirring for 5 h. Subsequently, the solution was heated to 120 ºC for evaporation and drying, and then calcined at 650 ºC for 6 h to obtain the FeMn/SiO_2 sample. Na/FeMn/ZrO_2 catalyst was prepared by impregnating method. Typically, Na_2CO_3 (AR, Sinopharm Chemical Reagent Co., Ltd) was dissolved into deionized water, and then the above solution was added dropwise to FeMn/SiO_2 sample under ultrasonic condition, followed by drying in vacuum at 60 ºC for 12 h to obtain Na/FeMn/SiO_2 catalyst. The weight percent of Na and FeMn are fixed at 2 wt% and 30 wt%, respectively.

The reference Na/FeMn catalyst were prepared by sol-gel method. Typically, a certain amount of $Fe(NO_3)_3{\cdot}9H_2O$, $Mn(NO_3)_2{\cdot}6H_2O$, and ethylene diamine tetraacetic acid were dissolved into deionized water to form uniform solution under stirring. After that, evaporation dried at 120 ºC under stirring, and then calcined at 650 ºC for 5 h to obtain FeMn samples. Na/FeMn catalyst was prepared by impregnating method. Na_2CO_3 was dissolved into deionized water, and then was dropped in the FeMn sample, dried at 60 ºC in vacuum for overnight. The final catalyst was denoted as Na/FeMn. The Fe and Na/Fe were prepared by the above-mentioned process.

2. Catalyst characterization

X-ray diffraction (XRD) spectra were performed on a Rigaku RINT 2400 X-ray diffract meter equipped using Cu Kα radiation at 40 kV and 20 mA with a scanning speed of 2 º·min^{-1} and step width of 0.02 º. *In situ* XRD analysis was conducted on a Rigaku SmartLab equipped with Cu Kα radiation. Samples were reduced in flowing H_2 (30 mL·min^{-1}) with programmed heating from room temperature to 600 ºC. To monitor catalyst phase evolution during the

reaction process, the catalyst was first reduced at 400 ºC for 1 h. After pretreatment, the sample was cooled down to 100 °C, followed by reaction gas introduction and data recording.

Scanning electron microscopy (SEM) images were taken on a JEOL JSM-6360LV microscope operated at an accelerating voltage of 1.5 kV. Transmission electron microscopy (TEM) and elemental mapping images were obtained on a JEOL JEM-2100F at an acceleration voltage of 200 kV.

N_2 sorption was conducted on a Micromeritics NOVA2200e analyzer. Prior to the measurement, the sample was degassed in vacuum at 200 ºC for 5 h. The surface area was calculated by the Brunauer-Emmett-Teller (BET) method. The average pore size and pore volume were determined by the Barrett-Joyner-Halenda (BJH) method.

Hydrogen temperature-programmed reduction (H_2-TPR) measurements were performed on a BELCAT-II-T-SP with a thermal conductivity detector (TCD). Specifically, 50 mg catalyst was loaded into a U-shaped quartz tube reactor and pretreated at 150 ºC for 2 h in flowing He. After that, the sample was cooled down to 100 °C, followed by reduction in flowing H_2 (30 $mL \cdot min^{-1}$) at 10 $^{\circ}C \cdot min^{-1}$ up to 600 °C.

Temperature-programmed desorption (TPD) was performed on a BELCAT-II-T-SP instrument with a TCD. Specifically, 50 mg sample was loaded into a quartz tube reactor and reduced at 400 $^{\circ}C$ for 2 h in flowing H_2 (30 $mL \cdot min^{-1}$). After that, the sample was cooled down to 50 $^{\circ}C$ and saturated with CO_2 or CO. The sample was flushed in flowing He for 0.5 h to remove the gaseous CO_2 or CO. Then, TPD was carried out in flowing He (30 $mL \cdot min^{-1}$) from 60 to 300 °C at 10 $°C \cdot min^{-1}$.

X-ray photoelectron spectroscopy (XPS) analysis was performed on a Thermo Fisher

Scientific ESCALAB 250Xi instrument using an Al Ka X-ray radiation source. The binding energy was calibrated by C 1s of adventitious carbon (284.6 eV).

The ^{57}Fe Mössbauer spectra (MES) were carried out on a wissel spectrometer driving with a proportional counter at room temperature. The radioactive source was ^{57}Co(Pd) moving in a constant acceleration mode. The components of iron phases were identified based on their Mössbauer parameters including isomer shift, quadruple splitting and magnetic hyperfine field.

H_2-temperature programmed surface reaction (H_2-TPSR) experiments were performed on a Micromeritics AutoChem II 2920 instrument. Specifically, the spent catalyst was purged with Ar at 320 °C for 1 h, followed by *in situ* reduction with H_2 for 1 h. After cooling to 50 °C, the catalyst was exposed to a 5%CO/Ar mixture gas for 30 min. The sample was then purged with Ar at 50 °C for 30 min. Subsequently, H_2 was introduced into the reactor with a programmed temperature ramp from 50 °C to 800 °C. Mass spectrometry (MS) signals for CO (m/z = 28) and H_2 (m/z = 2) were recorded.

In situ diffuse reflectance infrared fourier transform spectroscopy (DRIFTS) was performed on a Nicolet Nexus 470 FTIR spectrometer equipped with a diffuse reflectance attachment and a mercury cadmium telluride (MCT) detector. Prior to the test, 20 mg sample was placed in a diffuse reflectance infrared cell with a ZnSe window. The sample was reduced at 400 ºC for 1 h with a pure H_2 flow of 30 mL/min, and then cooled down to 320 ºC and the background spectrum was recorded. After the feedstock was introduced into the cell with flow of 30 mL/min, and the spectra were recorded by collecting 32 scans at 4 cm^{-1} resolution.

CO-DRIFTS was performed on a Nicolet 6700 spectrometer equipped with a diffuse reflectance cell and a liquid nitrogen-cooled high sensitivity MCT detector to detect the

adsorption and desorption of CO on the catalyst surface. The samples were first loaded into a reaction chamber and reduced by 10 % H_2/Ar at a flow rate of 30 mL·min^{-1} at 400 °C. Subsequently, 10 % CO/Ar was introduced into the reaction chamber and spectral data were collected.

3. DFT calculations

All calculations employed spin-polarized density functional theory (DFT) using the VASP software [1,2]. The exchange–correlation functional was treated within the generalized gradient approximation (GGA) using the Perdew-Burke-Ernzerhof (PBE) functional [3]. A plane-wave cutoff energy of 450 eV was applied. Valence electrons were described using the projector-augmented wave (PAW) method [4]. A Hubbard *U* correction of 5.0 eV was applied to the Ce 4f orbitals to accurately describe electron localization [5]. Ionic relaxation was performed until the maximum force on atom was below 0.05 eV/Å. van-der-Waals interactions were accounted for using the DFT-D3 method [6]. The bottom two atomic layers were fixed in position, while all other atoms were allowed to relax. Transition states were located using the climbing image nudge elastic band (CI-NEB) method. The results in Figure 7c and Figure 7d were obtained using this method.

4. Catalytic evaluation

CO_2 hydrogenation reactions were performed in a stainless steel fixed-bed reactor. In brief, 0.4 g catalyst was evenly mixed with 0.5 g quartz sand, which was then loaded in a reactor with internal diameter of 6 mm. Prior to reaction, the catalyst was *in situ* reduced at 400 ºC for 8 h in flowing H_2 (60 mL·min^{-1}) at atmospheric pressure. After reduction, the catalyst was cooled down to 320 ºC, and then the reactant gas mixture (gas composition as 25.03 % CO_2, 70.0 %

H_2, Ar balance) was fed into the reactor. The reaction was carried out at 320 ºC, 1.5 MPa, and 7500 $mL \cdot g_{cat}^{-1} \cdot h^{-1}$. Reaction effluents were quantitatively analyzed using online gas chromatograph (GC-2014C, Shimadzu) equipped with TCD and active charcoal column (TDX-01) for Ar, CO, CH_4, and CO_2 analysis together with flame ionization detector (FID) and Rtx-1 capillary column (60 m × 0.32 mm × 5 μm) for hydrocarbon analysis. The hydrocarbon distribution was calculated from total carbon moles.

CO_2 conversion and CO selectivity were calculated as follows:

$$CO_2 \text{ conversion} = \frac{CO_{2\ inlet} - CO_{2\ outlet}}{CO_{2\ inlet}} \times 100\% \quad (1)$$

$$\text{CO selectivity} = \frac{CO_{outlet}}{CO_{2\ inlet} - CO_{2\ outlet}} \times 100\% \quad (2)$$

where, CO_2 inlet, CO_2 outlet, and CO outlet represent the moles of CO_2 at the inlet and outlet, and the moles of CO at the outlet, respectively.

The selectivity of hydrocarbon in total hydrocarbons was calculated as follows:

$$C_i \text{ hydrocarbon selectivity} = \frac{mole\ of\ Ci\ hydrocarbon \times i}{\sum_{i=1}^{n} mole\ of\ Ci\ hydrocarbon \times i} \times 100\ \% \quad (3)$$

5. Results and discussion

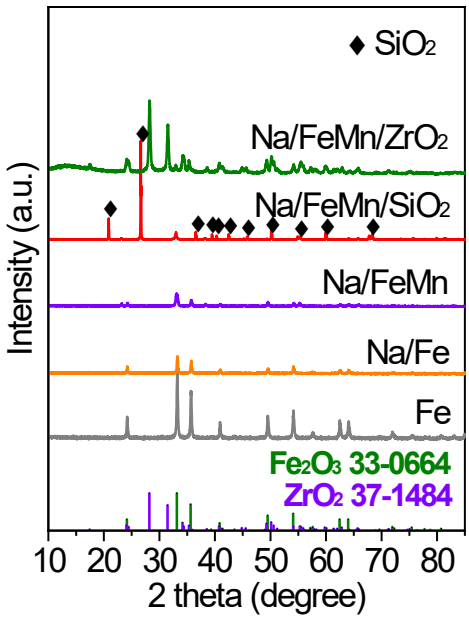

Figure S1. XRD patterns of the fresh catalysts

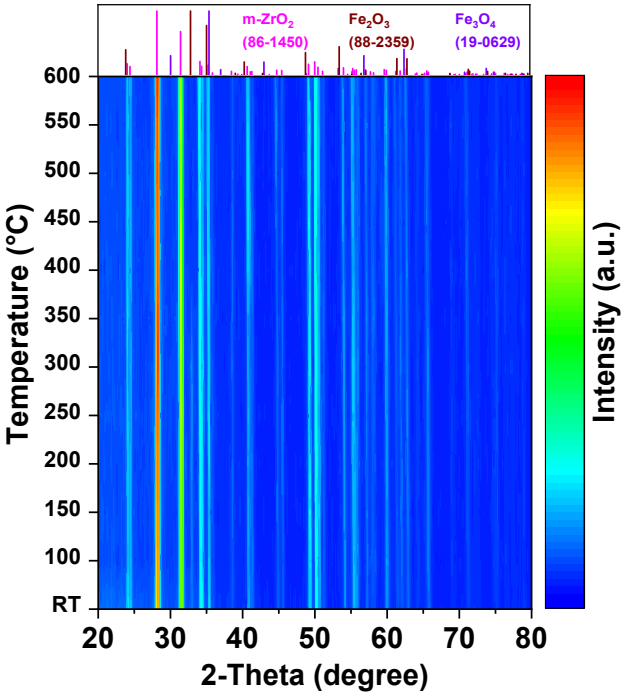

Figure S2. *In situ* XRD patterns of the Na/FeMn/ZrO_2 catalyst for H_2 reduction process.

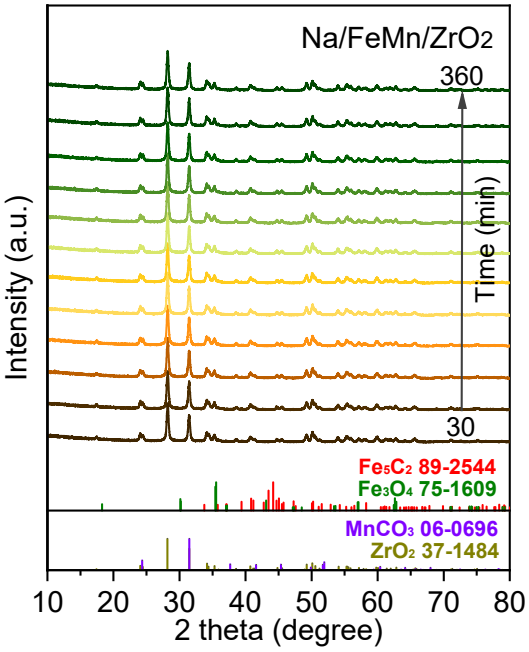

Figure S3. *In situ* XRD patterns of Na/FeMn/ZrO_2 for CO_2 hydrogenation.

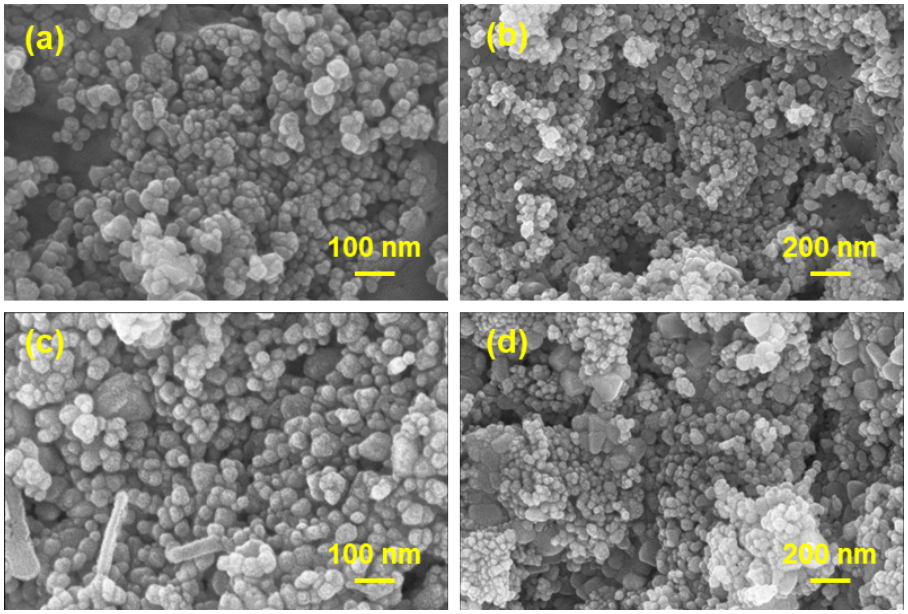

Figure S4. SEM images of the fresh Na/FeMn/ZrO_2 (a,b) and spent Na/FeMn/ZrO_2 (c,d) catalyst.

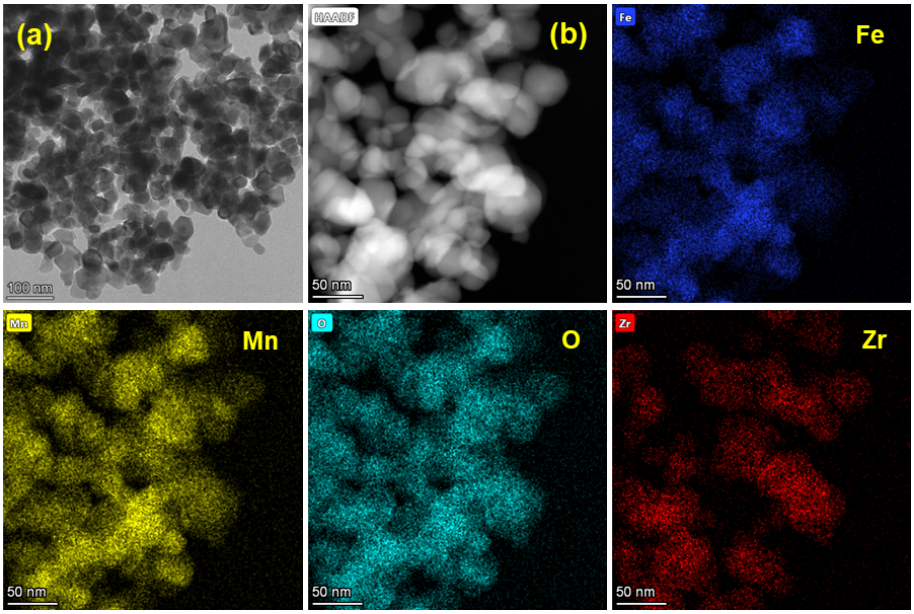

Figure S5. TEM image (a), STEM image (b) and EDS elemental mapping images of the fresh Na/FeMn/ZrO_2 catalyst.

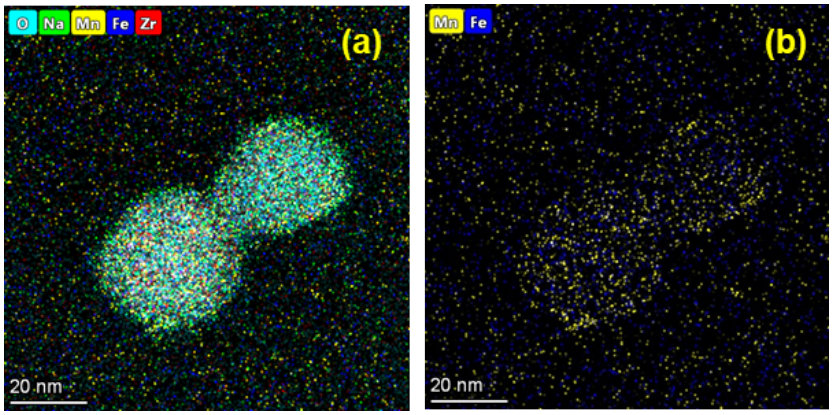

Figure S6. The EDS mapping images of (a) all elemental, (b) Fe and Mn in the spent Na/FeMn/ZrO_2 catalyst

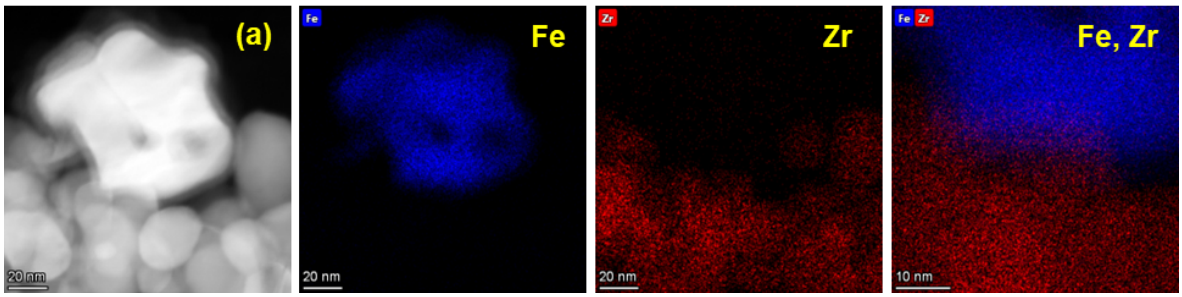

Figure S7. STEM image of spent Na/FeMn/ZrO_2 catalyst (a), EDS mapping images of all elemental (b), and the corresponding EDS elemental mapping images.

Table S1. The elemental composition of the as-prepared catalysts.

Catalysts	Element content (wt%) [a]				Dosage of raw materials (wt%) [b]			
	Na	Fe	Mn	Si or Zr	Na	Fe	Mn	Si or Zr
Na/FeMn	1.7	21.6	20.9	/	2.0	22.8	19.6	/
Na/FeMn/SiO_2	1.7	4.7	3.5	37.4	2.0	3.6	3.1	39.1
Na/ FeMn/ZrO_2	1.9	3.8	4.0	61.5	2.0	3.6	3.1	62.3

[a]The elemental composition of these catalysts was obtained by ICP analysis.

[b]The dosages of the elements were calculated according to the amounts of raw materials in the catalyst preparation.

Table S2. Textural properties of the prepared catalysts.

Catalysts	BET surface area[a] ($m^2 \cdot g^{-1}$)	Pore volume[b] ($cm^3 \cdot g^{-1}$)	Average pore size[c] (nm)
Fe	23.7	0.14	11.5
Na/Fe	25.0	0.20	13.8
Na/FeMn	17.2	0.14	12.3
Na/FeMn/SiO_2	14.7	0.04	1.7
Na/FeMn/ZrO_2	31.5	0.26	8.7

[a]BET specific surface area; [b]pore volume calculated by BJH method; [c]average diameter of mesopores evaluated by the BJH method.

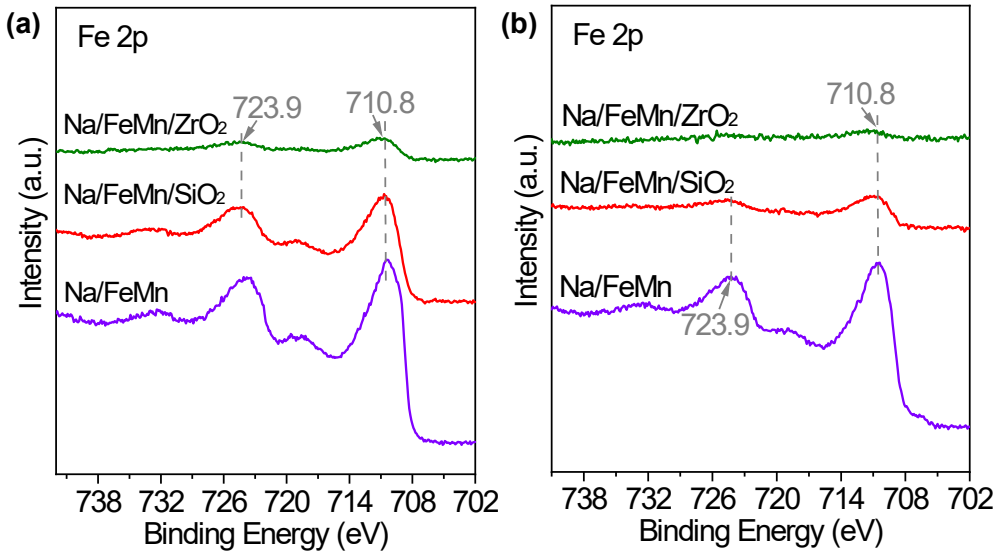

Figure S8. Fe 2p XPS spectra of fresh (a) and reduced (b) catalysts.

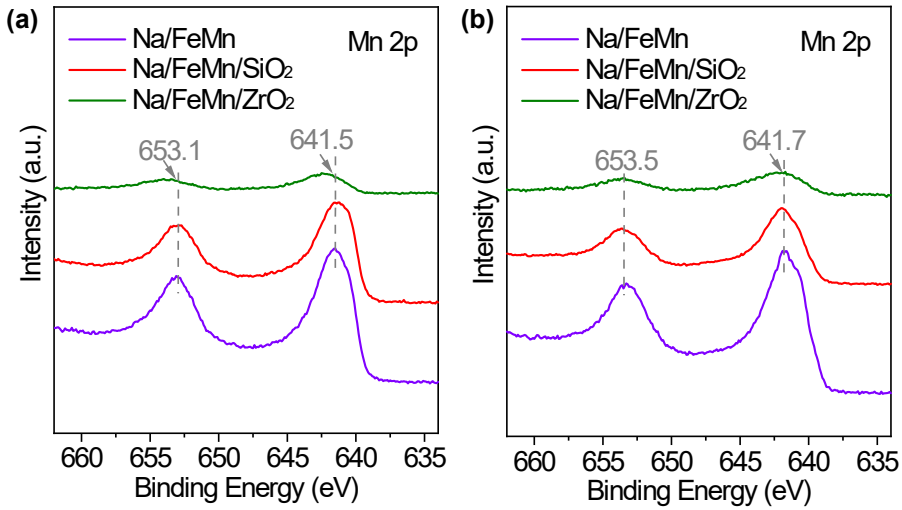

Figure S9. Mn 2p XPS spectra of fresh (a) and reduced (b) catalysts.

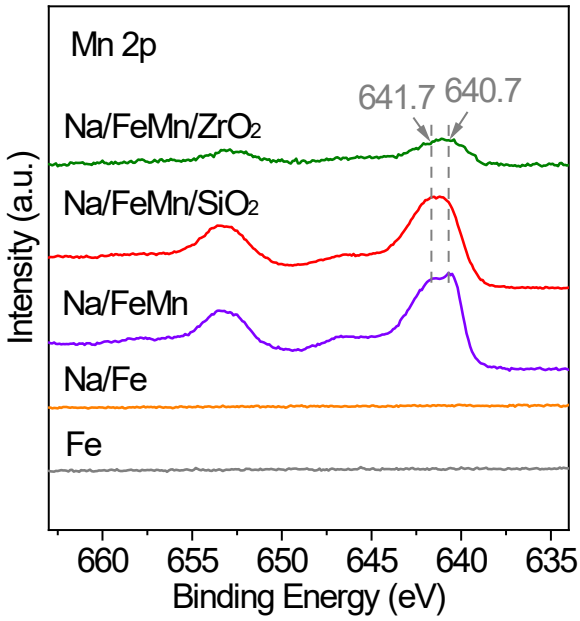

Figure S10. Mn 2p XPS spectra of the spent catalysts.

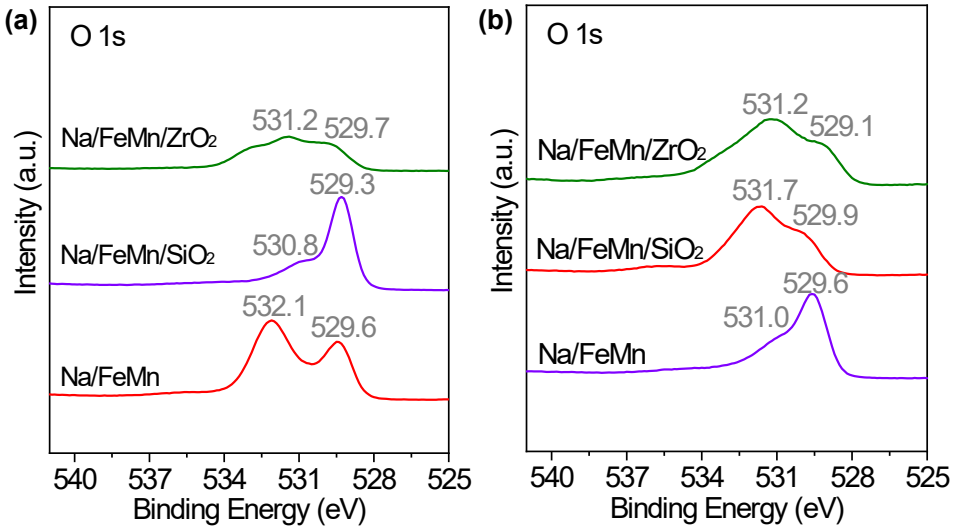

Figure S11. O 1s XPS spectra of fresh (a) and reduced (b) catalysts.

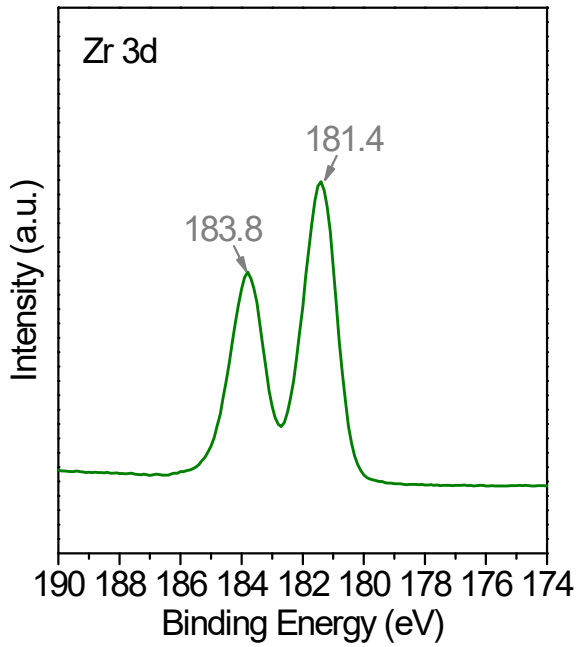

Figure S12. Zr 3d XPS spectra of the spent Na/FeMn/ZrO_2 catalyst.

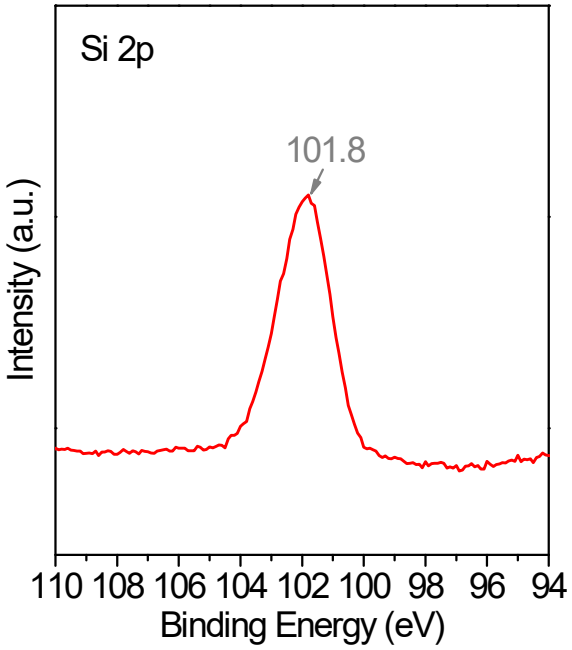

Figure S13. Si 2p XPS spectra of the spent Na/FeMn/SiO_2 catalyst.

Table S3. Surface element content of the spent catalysts obtained by XPS analysis.

Sample	Elements contents (%)					
	Fe	C	O	Na	Mn	Si or Zr
Fe	31.4	21.1	47.5	/	/	/
Na/Fe	21.7	36.5	34.1	7.7	/	/
Na/FeMn	7.1	31.7	39.7	8.4	13.1	/
Na/FeMn/SiO_2	7.8	26.9	40.7	7.9	11.0	5.7
Na/FeMn/ZrO_2	8.1	30.8	36.8	8.2	9.8	6.3

[a] Calculated in atomic %.

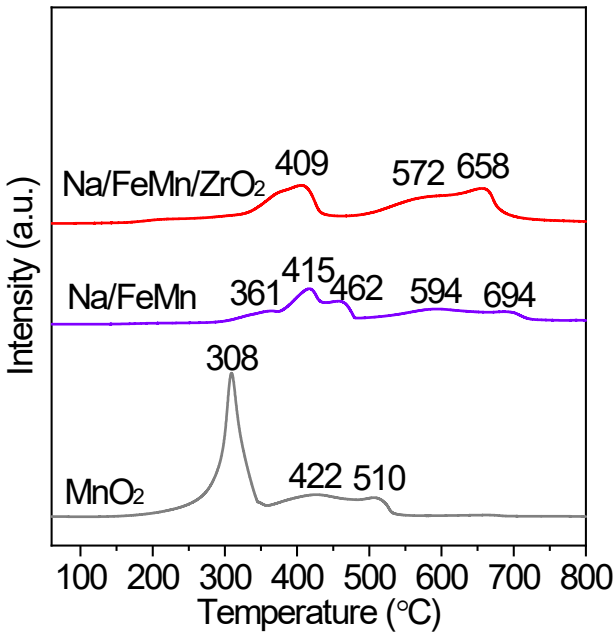

Figure S14. H_2-TPR profiles of the reference MnO_2, Na/FeMn, and Na/FeMn/ZrO_2 catalysts.

Table S4. The H_2 consumption of the prepared catalyst during the H_2 reduction process

Catalysts	T_m (°C) [a]			H_2 consumption (μmol·g^{-1}) [b]		
	α	β	γ	α	β	γ
Fe	50-380	380-600	600-800	3400.5	7280.1	0
Na/Fe	50-450	450-590	590-800	1899.2	8977.0	1237.4
Na/FeMn	50-480	480-660	660-800	3744.2	2360.7	1197.2
Na/FeMn/SiO_2	50-480	480-600	600-800	374.1	653.2	523.4
Na/FeMn/ZrO_2	50-460	460-610	610-800	514.0	347.2	359.1

[a] Temperature range of the reduction peak.

[b] The H_2 consumption of these catalysts was obtained by H_2-TPR analysis.

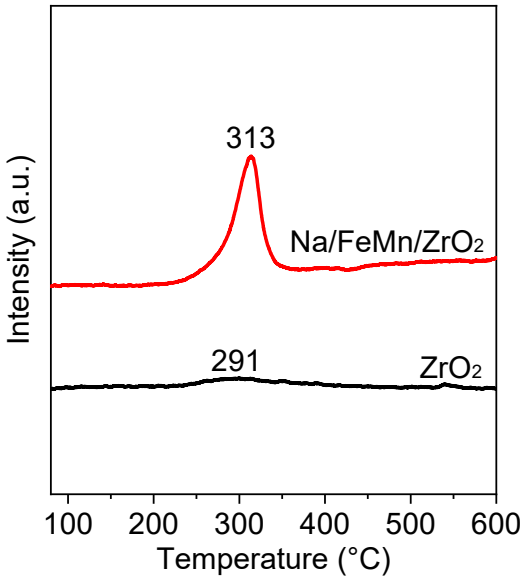

Figure S15. CO-TPD profiles of the reference ZrO_2 and Na/FeMn/ZrO_2 catalysts.

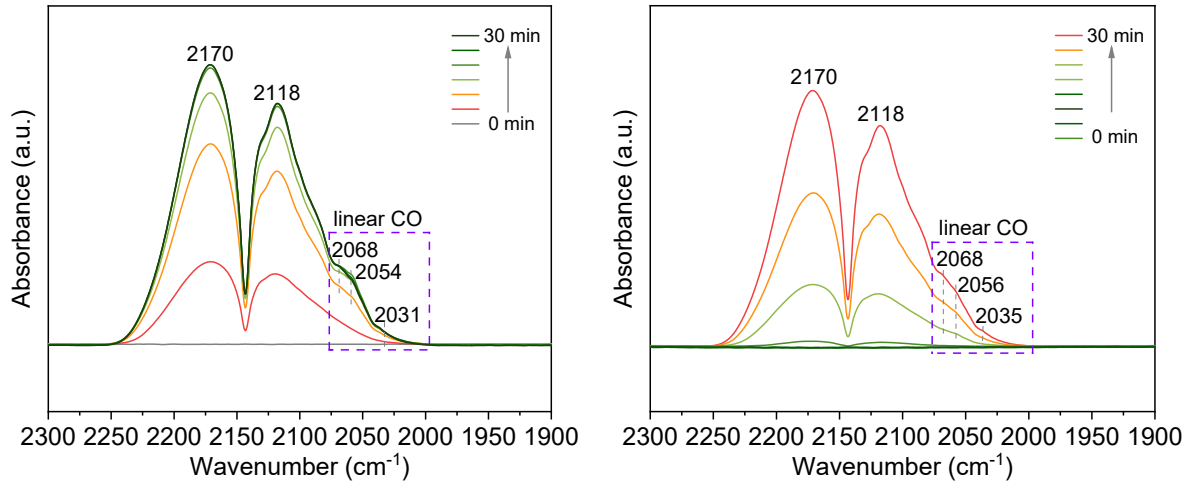

Figure S16. DRIFTS of CO adsorption (a) and CO desorption (b) spectra of Na/FeMn/ZrO_2 catalyst.

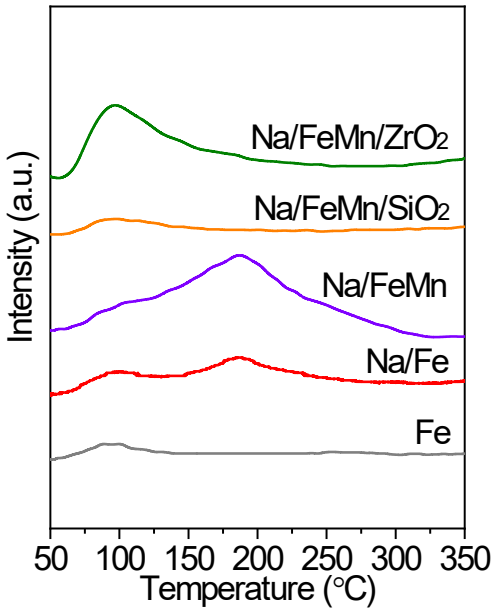

Figure S17. CO_2-TPD profiles of the catalysts.

Table S5. Detailed Mössbauer parameters

Catalyst	Assignment	Mössbauer parameters				
		IS ($mm \cdot s^{-1}$)	QS ($mm \cdot s^{-1}$)	H (T)	Γ ($mm \cdot s^{-1}$)	Area (%)
Na/FeMn/ZrO_2-spent	Fe_3O_4(B)	0.4	-0.05	48.56	0.19	1.3
	Fe_3O_4(A)	0.79	0.01	49.12	0.23	2.5
	χ-Fe_5C_2(II)	0.08	0.05	19.88	0.55	31.7
	χ-Fe_5C_2(I)	0.15	0.16	22.48	0.48	26.2
	χ-Fe_5C_2(III)	0.07	0.18	11.79	0.32	21.7
	Fe^{3+}	0.24	0.85	—	0.88	16.6

Table S6. Catalytic performance for the hydrogenation CO_2 to long chain linear α-olefins.

Catalysts	CO_2 conv. (%)	CO sel. (%)	Hydrocarbon distribution (%)					LAOs sel. (%)	LAOs /C_{4+} (%)	O/P	LAOs yield (%)
			CH_4	C_{2-4}^0	$C_{2-4}^=$	C_{5+}^0	$C_{5+}^=$				
Fe	29.3	21.4	38.2	46.6	3.8	11.3	0.2	0.9	4.1	0.1	0.2
Na/Fe	33.6	22.0	13.7	8.9	31.3	29.6	16.5	25.0	42.5	3.5	6.5
Na/FeMn	30.2	31.9	12.7	9.1	35.9	21.4	21.0	31.0	54.8	4.0	6.3
Na/FeMn/SiO_2	18.3	48.3	51.0	24.7	10.2	14.1	0.1	1.0	4.6	0.4	0.1
Na/FeMn/ZrO_2	29.4	23.0	18.5	8.9	43.3	11.3	17.9	29.6	68.0	5.1	6.7

Reaction conditions: H_2/CO_2 = 3, 1.5 MPa, 320 °C, WHSV=7500 $mL \cdot g_{cat}^{-1} \cdot h^{-1}$, TOS = 10 h

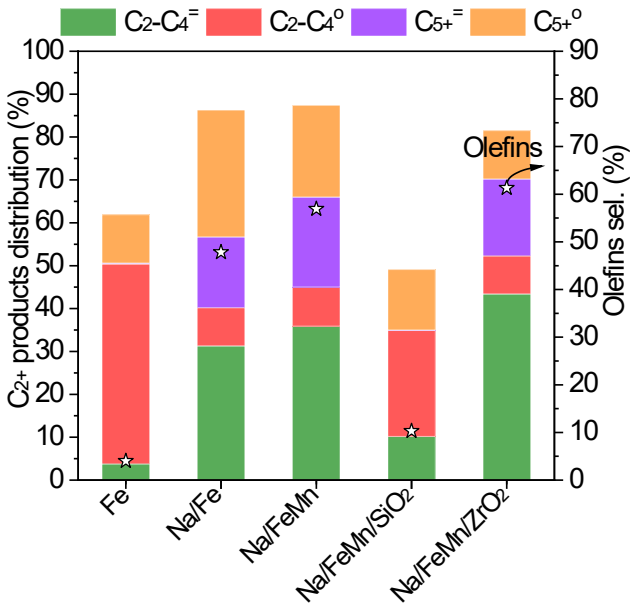

Figure S18. C_{2+} products distribution and olefins selectivity. Reaction conditions: H_2/CO_2 = 3, 1.5 MPa, 320 ºC, 7500 mL·gcat^{-1}·h^{-1}, TOS = 10 h.

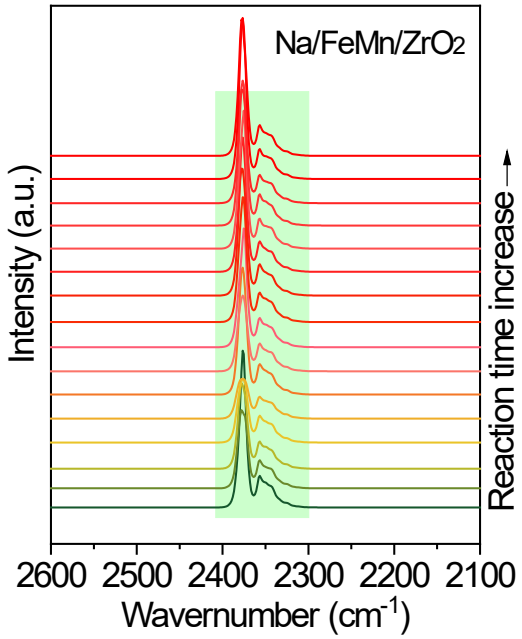

Figure S19. *In situ* DRIFTS of CO_2 hydrogenation to LAOs over the Na/FeMn/ZrO_2 catalyst. Reduced conditions: 400 ºC, H_2, 30 mL·min^{-1}; Reaction conditions: H_2/CO_2 = 3, 320 ºC, 30 mL·min^{-1}.

Figure S20. Adsorption model of CH_2+CH_2 over Fe_5C_2 and the Fe_5C_2-ZrO_2 interface.

References

[1] Kresse, G.; Furthmüller, J. Efficiency of Ab-Initio Total Energy Calculations for Metals and Semiconductors Using a Plane-Wave Basis Set. Computational Materials Science, 1996, 6, 15–50.

[2] Kresse, G.; Furthmüller, J. Efficient Iterative Schemes for Ab Initio Total-Energy Calculations Using a Plane-Wave Basis Set. Physical Review B, 1996, 54, 11169–11186.

[3] Perdew, J. P.; Burke, K.; Ernzerhof, M. Generalized Gradient Approximation Made Simple. Physical Review Letters, 1996, 77, 3865–3868.

[4] Kośmider, K.; Brázdová, V.; Ganduglia-Pirovano, M. V.; Pérez, R. Do Au Atoms Titrate Ce^{3+} Ions at the CeO_{2-x} (111) Surface? The Journal of Physical Chemistry C, 2016, 120, 927–933.

[5] Grimme, S.; Antony, J.; Ehrlich, S.; Krieg, H. A Consistent and Accurate Ab Initio Parametrization of Density Functional Dispersion Correction (DFT-D) for the 94 Elements H-Pu. The Journal of Chemical Physics, 2010, 132.

[6] Henkelman, G.; Uberuaga, B. P.; Jónsson, H. A Climbing Image Nudged Elastic Band Method for Finding Saddle Points and Minimum Energy Paths. The Journal of Chemical Physics, 2000, 113, 9901–9904.